Journal of Cellular Biochemistry 104:862–878 (2008)

Apoptosis in Arsenic Trioxide-Treated Calu-6 Lung Cells Is Correlated With the Depletion of GSH Levels Rather Than the Changes of ROS Levels

Yong Hwan Han, Suhn Hee Kim, Sung Zoo Kim, and Woo Hyun Park*

Department of Physiology, Medical School, Research Institute of Clinical Medicine, Centers for Healthcare Technology Development, Chonbuk National University, JeonJu 561-180, Republic of Korea

Abstract Arsenic trioxide (ATO) can regulate many biological functions such as apoptosis and differentiation in various cells. We investigated an involvement of ROS such as H_2O_2 and $O_2^{\cdot -}$, and GSH in ATO-treated Calu-6 cell death. The levels of intracellular H_2O_2 were decreased in ATO-treated Calu-6 cells at 72 h. However, the levels of $O_2^{\cdot -}$ were significantly increased. ATO reduced the intracellular GSH content. Many of the cells having depleted GSH contents were dead, as evidenced by the propidium iodine staining. The activity of CuZn-SOD was strongly down-regulated by ATO at 72 h while the activity of Mn-SOD was weakly up-regulated. The activity of catalase was decreased by ATO. ROS scavengers, Tiron and Trimetazidine did not reduce levels of apoptosis and intracellular $O_2^{\cdot -}$ in ATO-treated Calu-6 cells. Tempol showing a decrease in intracellular $O_2^{\cdot -}$ levels reduced the loss of mitochondrial transmembrane potential ($\Delta\Psi_m$). Treatment with NAC showing the recovery of GSH depletion and the decreased effect on $O_2^{\cdot -}$ levels in ATO-treated cells significantly inhibited apoptosis. In addition, BSO significantly increased the depletion of GSH content and apoptosis in ATO-treated cells. Treatment with SOD and catalase significantly reduced the levels of $O_2^{\cdot -}$ levels in ATO-treated cells, but did not inhibit apoptosis along with non-effect on the recovery of GSH depletion. Taken together, our results suggest that ATO induces apoptosis in Calu-6 cells via the depletion of the intracellular GSH contents rather than the changes of ROS levels. J. Cell. Biochem. 104: 862–878, 2008.

Key words: arsenic trioxide; ROS; GSH; apoptosis; mitochondria; Calu-6

Reactive oxygen species (ROS) include hydrogen peroxide (H_2O_2), superoxide anion ($O_2^{\cdot -}$), and hydroxyl radical ($^{\cdot}OH$). These molecules have recently been implicated in the regulation of many important cellular events, including transcription factor activation, gene expression, differentiation, and cellular proliferation [Baran et al., 2004; Bubici et al., 2006]. ROS are formed as by-products of mitochondrial respiration or oxidases, including nicotine adenine diphosphate (NADPH) oxidase, xanthine oxidase (XO), and certain arachidonic acid oxygenases [Zorov et al., 2006]. A change in the redox state of the tissue implies a change in ROS generation or metabolism. Principal metabolic pathways include superoxide dismutase (SOD), which is expressed as extracellular, intracellular, and mitochondrial isoforms. These isoforms metabolize $O_2^{\cdot -}$ to H_2O_2. Further metabolism by peroxidases that include catalase and glutathione (GSH) peroxidase yields O_2 and H_2O [Wilcox, 2002]. GSH is a main non-protein antioxidant in the cell and it can clear away

This article contains supplementary material, which may be viewed at the Journal of Cellular Biochemistry website at http://www.interscience.wiley.com/jpages/0730-2312/suppmat/index.html.

Abbreviations used: ATO, arsenic trioxide; ROS, reactive oxygen species; NADPH, nicotine adenine diphosphate; XO, xanthine oxidase; SOD, superoxide dismutase; FBS, fetal bovine serum; PBS, phosphate buffer saline; FITC, fluorescein isothiocyanate; H_2DCFDA, 2′,7′-Dichlorodihydrofluorescein diacetate; DHE, dihydroethidium; GSH, glutathione; NAC, *N*-acetylcysteine; CMFDA, 5-chloromethylfluorescein diacetate; PI, propidium iodide; BSO, L-buthionine sulfoximine.

The authors declare that there are no possible conflicts of interest in this paper.

Grant sponsor: Korean Science and Engineering Foundation; Grant number: R01-2006-000-10544-0.

*Correspondence to: Woo Hyun Park, PhD, Assistant Professor, Department of Physiology, Medical School, Chonbuk National University, JeonJu 561-180, Republic of Korea. E-mail: parkwh71@chonbuk.ac.kr

Received 12 May 2007; Accepted 26 November 2007

DOI 10.1002/jcb.21673

the superoxide anion free radical and provide electrons for enzymes such as glutathione peroxidase, which reduce H_2O_2 to H_2O. GSH has been shown to be crucial for regulation of cell proliferation, cell cycle progression and apoptosis [Poot et al., 1995; Schnelldorfer et al., 2000] and is known to protect cells from toxic insult through detoxification of toxic metabolites of drugs and ROS [Lauterburg, 2002]. Although cells possess antioxidant systems to control the redox state, which is important for their survival, excessive production of ROS can be induced and gives rise to the activation of events that lead to death or survival in several cell types [Simon et al., 2000; Chen et al., 2006; Dasmahapatra et al., 2006; Wallach-Dayan et al., 2006]. The exact mechanisms involved in cell death induced by ROS are not fully understood and the protective effect mediated by some antioxidants remains controversial.

Arsenic trioxide (ATO; As_2O_3) has been firstly reported to induce complete remission in patients with relapsed or refractory acute promyelocytic leukemia (APL) without severe marrow suppression [Soignet et al., 1998]. The antiproliferative effect of ATO is not limited to APL cells, but can also be observed in a variety of hematological malignancies [Wang et al., 1998; Zhang et al., 1998; Park et al., 2000]. Accumulating evidences have indicated that ATO can regulate many biological functions such as cell proliferation, apoptosis, differentiation, and angiogenesis in various cell lines such as renal [Hyun Park et al., 2003], head and neck [Seol et al., 1999], ovarian [Uslu et al., 2000], prostate [Uslu et al., 2000], hepatoma [Kito et al., 2002; Oketani et al., 2002], bladder [Pu et al., 2002], colon [Nakagawa et al., 2002], lung [Li et al., 2002], breast [Baj et al., 2002], cervical [Woo et al., 2002], and gastric [Zhang et al., 1999] cancer cells. ATO as a mitochondrial toxin induces a loss of mitochondrial transmembrane potential [Park et al., 2000; Hyun Park et al., 2003; Haga et al., 2005] and, as such, it induces the generation of ROS [Miller et al., 2002; Kim et al., 2006; Li et al., 2006]. These phenomena could trigger the apoptosis of target cells. Therefore, it is thought that ATO induces apoptosis in tumor cells by affecting the mitochondria and ROS generation. In addition, it has been reported that the intracellular GSH content has a decisive effect on ATO-induced apoptosis [Dai et al., 1999; Kitamura et al., 2000; Wu et al., 2004; Li et al., 2006]. Furthermore, a combination of ATO and L-buthionine sulfoximine (BSO; an inhibitor of GSH synthesis) induced synergistic cytotoxicity in several cell lines of renal cell carcinoma [Wu et al., 2004], bladder cancer [Pu et al., 2002], leukemia [Dai et al., 1999], hepatocellular carcinoma [Kito et al., 2002], and solid tumors [Maeda et al., 2004].

We have recently found that that ATO inhibited the growth of Calu-6 cells with an IC_{50} of about 3–4 μM at 72 h. Treatment with 10 μM ATO efficiently induced apoptosis, as evidenced by flow cytometric detection of sub-G1 DNA content, annexin V binding assay and DAPI staining. This apoptotic process was accompanied by the loss of mitochondrial membrane potential ($\Delta\Psi_m$), Bcl-2 down- regulation, the activation of caspase-3 and PARP degradation (unpublished data). In the present study, we evaluated the involvement of ROS and GSH in ATO-induced Calu-6 cell death, investigated whether ROS scavengers could rescue Calu-6 cells from ATO-induced death and described its mechanism in relation to ROS and GSH.

MATERIALS AND METHODS

Cell Culture

Human lung adenocarcinoma Calu-6 and A549 cells were maintained in humidified room air containing 5% CO2 at 37°C. Cells were cultured in RPMI-1640 supplemented with 10% fetal bovine serum (FBS) and 1% penicillin-streptomycin (GIBCO BRL, Grand Island, NY). Cells were routinely grown in 100-mm plastic tissue culture dishes (Nunc, Roskilde, Denmark) and harvested with a solution of trypsin-EDTA while in a logarithmic phase of growth. Cells were maintained at these culture conditions for all experiments.

Reagents

ATO and BSO (L-buthionine sulfoximine) were purchased from Sigma–Aldrich Chemical Company (St. Louis, MO) and were dissolved in 1.65 M NaOH and distilled water at 1×10^{-1} M as a stock solution, respectively. The cell-permeable $O_2^{\cdot -}$ scavengers, 4-hydroxy-TEMPO (4-hydroxyl-2,2,6,6-tetramethylpierydine-1-oxyl) (Tempol), 4,5-dihydroxyl-1,3-benzededisulfonic acid (Tiron), 1-[2,3,4-trimethoxibenzyl]-piperazine (Trimetazidine), reduced-GSHester (rGSHester) and N-acetylcysteine (NAC) were obtained from

Sigma. These were dissolved in designated solution buffer (ethanol or water) at 1×10^{-1} M as a stock solution. SOD and catalase were obtained from Sigma and dissolved in 50 mM potassium phosphate buffer at 4733 U/ml. One unit of SOD and catalase is defined as the amount of enzyme needed to Exhibit 50% dismutation of the superoxide radical and to Exhibit 50% decomposition of hydrogen peroxide to oxygen and water, respectively. All of the stock solutions were wrapped in foil and kept at 4°C or −20°C.

Detection of the Intracellular H_2O_2 and $O_2^{\cdot -}$ Concentration

The intracellular H_2O_2 concentration was detected by means of an oxidation-sensitive fluorescent probe dye, 2′,7′-Dichlorodihydrofluorescein diacetate (H_2DCFDA) (Invitrogen Molecular Probes, Eugene, OR). H_2DCFDA was intracellularly deacetylated by non-specific esterase, which was further oxidized by cellular peroxides to the fluorescent compound, 2, 7-dichlorofluorescein (DCF) (Ex/Em = 495 nm/529 nm). Dihydroethidium (DHE) (Ex/Em = 518 nm/605 nm) (Invitrogen Molecular Probes) is a fluorogenic probe that is highly selective for superoxide anion radical detection. DHE is cell-permeable and reacts with superoxide anion to form ethidium, which, in turn, intercalates in the deoxyribonucleic acid, thereby exhibiting a red fluorescence. In brief, cells were incubated with ATO with or without ROS scavengers or BSO for 72 h or for the indicated amounts of time. Cells were then washed with PBS and incubated with 20 μM H_2DCFDA or 5 μM DHE at 37°C for 30 min according to the instructions of the manufacturer. DCF fluorescence and red fluorescence were detected using a FACStar flow cytometer (Becton Dickinson, San Jose, CA). For each sample, 5,000 or 10,000 events were collected. H_2O_2 and $O_2^{\cdot -}$ production were expressed as mean fluorescence intensity (MFI), which was calculated by CellQuest software.

Detection of the Intracellular Glutathione (GSH)

Cellular GSH levels were analyzed using 5-chloromethylfluorescein diacetate (CMFDA, Molecular Probes). CMFDA (Ex/Em = 492 nm/517 nm) is a useful, membrane-permeable dye for determining levels of the intracellular glutathione [Hedley and Chow, 1994; Macho et al., 1997]. In brief, cells were incubated with the ATO with or without ROS scavenger or BSO for 72 h or for the amounts of time. Cells were then washed with PBS and incubated with 5 μM CMFDA at 37°C for 30 min according to the instructions of the manufacturer. Cytoplasmic esterases convert non-fluorescent CMFDA to fluorescent 5-chloromethylfluorescein, which can then react with the glutathione. PI can be used to differentiate necrotic, apoptotic and normal cells. This agent is membrane impermeant and generally excluded from viable cells. PI (1 μg/ml) was subsequently added, and CMF fluorescence and PI (Ex/Em = 488 nm/617 nm) staining intensity were determined using a FACStar flow cytometer (Becton Dickinson) and calculated by CellQuest software. For each sample, 5,000 or 10,000 events were collected.

Measurement of Cellular Catalase Activity

The level of cellular catalase enzyme activity was measured using a catalase assay kit from Sigma–Aldrich Chemical Company. In brief, cells were incubated with the designated dose of ATO for 72 h. The cells were washed with PBS and suspended in 5 volumes of lysis buffer (20 mM HEPES [pH 7.9], 20% Glycerol, 200 mM KCl, 0.5 mM EDTA, 0.5% NP40, 0.5 mM DTT, 1% protease inhibitor cocktail (from Sigma)). The lysates were then collected and stored at −20°C until further use. The supernatant protein concentration was determined by the Bradford method. Supernatant samples containing 30 μg of total protein were used for determination of catalase enzyme activity. These were added to a microcentrifuge tube with the appropriate volume of assay buffer (50 mM KH_2PO_4/50 mM Na_2HPO_4, pH 7.0). The reaction was initiated by the addition of 200 mM H_2O_2 solution at 25°C for 5 min, and was finished by the addition of stop solution. A small amount of the above reaction mixture was removed, added to another microcentrifuge tube with the color reagent (150 mM potassium phosphate buffer, pH7.0, containing 0.25 mM 4-aminoantipyrine, 2 mM 3,5-dichloro-2-hydroxybenzenesulfonic acid, and the peroxidase solution), and were incubated to convert the color reagent to a red quinoneimine color at 25°C for approximately 10 min. The dye was measured at 520 nm using a microplate reader (Spectra MAX 340, Molecular Devices Co, Sunnyvale, CA). A standard curve of catalase solution (5 U to 50 U/ml) was run for quantification.

Measurement of Cellular Superoxide Dismutase Activity

The levels of cellular SOD enzyme activity were measured using a SOD Assay Kit-WST (Fluka Co, Milwaukee), which allows very convenient SOD assaying by utilizing a highly water-soluble tetrazolium salt, WST-1 (2-(4-lodophenyl)-3-(4-nitrophenyl)-5-(2,4-disulfophenyl)-2H-tetrazolium, monosodium salt), which produces a water-soluble formazan dye upon reduction with a superoxide anion. In brief, cells were incubated with the designated dose of ATO for 72 h. The cells were washed in PBS and suspended in 5 volumes of lysis buffer (20 mM HEPES [pH 7.9], 20% Glycerol, 200 mM KCl, 0.5 mM EDTA, 0.5% NP40, 0.5 mM DTT, 1% protease inhibitor cocktail (from Sigma)). The lysates were then collected and stored at −20°C until further use. The supernatant protein concentration was determined by the Bradford method. Supernatant samples containing 30 μg of total protein were used for determination of SOD enzyme activity. These were added to each well in 96-well microtiter plates (Nunc) with WST working solution and enzyme working solution, and were incubated to produce a water-soluble formazan dye at 25°C for 10 min. The WST-1 formazan was measured at 450 nM using a microplate reader (Spectra MAX 340, Molecular Devices Co). Activities between Mn-SOD and Cu/Zn-SOD were distinguished by differential sensitivity to 1 mM potassium cyanide [Rigo et al., 1977]. A standard curve of SOD solution (5 U to 50 U/ml) was run for quantification.

Cell Viability Assay

The in vitro cell viability effect of ATO with or without BSO on Calu-6 cells was determined by measuring 3-(4,5-dimethylthiazol-2-yl)-2,5-diphenyltetrazolium bromide (MTT) dye absorbance of living cells as described previously [Park et al., 2000]. In brief, cells (2×10^5 cells per well) were seeded in 96-well microtiter plates in the presence of the designated doses of ATO with or without BSO (Nunc). After exposure to the drugs for 72 h, 50 μl of MTT (Sigma) solution (2 mg/ml in PBS) were added to each well, and the plates were incubated for an additional 3 or 4 h at 37°C. MTT solution in medium was removed following centrifugation of the plates. To achieve solubilization of the formazan crystals formed in viable cells, 100 or 200 μl of DMSO were added to each well. The optical density of each well was measured at 570 nm using a microplate reader (Spectra MAX 340, Molecular Devices Co). Each plate contained multiple wells at a given experimental condition and multiple control wells. This procedure was replicated for 2–4 plates/condition.

Sub-G_1 Analysis

The sub-G_1 distribution were determined by staining DNA with propidium iodide (PI; Sigma–Aldrich) as described previously [Park et al., 2000]. PI is a fluorescent biomolecule that can be used to stain DNA. In brief, 1×10^6 cells were incubated with the designated dose of ATO with or without ROS scavenger or BSO for 72 h. Cells were then washed with phosphate-buffered saline (PBS) and fixed in 70% ethanol. Cells were washed again with PBS and then incubated with PI (10 μg/ml) with simultaneous treatment of RNase at 37°C for 30 min. The percentages of cells containing sub-G_1 DNA content were measured using a FACStar flow cytometer (Becton Dickinson) and analyzed using lysis II and CellFIT software (Becton Dickinson) or ModFit software (Verity Software, Inc.).

Annexin V/PI Staining

Apoptosis was determined by staining cells with annexin V-fluorescein isothiocyanate (FITC) (Ex/Em = 495 nm/529 nm) and PI labeling, because annexin V can be used to identify the externalization of phosphatidylserine during the progression of apoptosis and, therefore, can detect cells during early phases of apoptosis. In brief, 1×10^6 cells were incubated with ATO with or without ROS scavenger or BSO for 72 h. The prepared cells were washed twice with cold PBS and then resuspended in 500 μl of binding buffer (10 mM HEPES/NaOH pH 7.4, 140 mM NaCl, 2.5 mM $CaCl_2$) at a concentration of 1×10^6 cells/ml. Five microliter of annexin V-FITC (PharMingen, San Diego, CA) and PI (1 μg/ml) were then added to these cells, which were analyzed with a FACStar flow cytometer (Becton Dickinson). Viable cells were negative for both PI and annexin V; apoptotic cells were positive for annexin V and negative for PI, whereas late apoptotic dead cells displayed both high annexin V and PI labeling. Non-viable cells, which underwent necrosis, were positive for PI and negative for annexin V.

Measurement of Mitochondrial Membrane Potential ($\Delta\Psi_m$)

Mitochondrial membrane was monitored using the fluorescent dye, Rhodamine 123 (Ex/Em = 507 nm/529 nm), a cell permeable cationic dye that preferentially enters into mitochondria based on highly negative mitochondrial membrane potential ($\Delta\Psi_m$). Depolarization of mitochondrial membrane potential ($\Delta\Psi_m$) results in the loss of Rhodamine 123 from the mitochondria and a decrease in the intracellular fluorescence. In brief, 1×10^6 cells were incubated with ATO with or without ROS scavenger or BSO for 72 h. Cells were washed twice with PBS and incubated with Rhodamine 123 (0.1 μg/ml; Sigma) at 37°C for 30 min. The percentages of cells containing Rhodamine 123 negative staining were determined by flow cytometry.

Statistical Analysis

Results represent the mean of at least three independent experiments; bar, SD. Microsoft Excel or Instat software (GraphPad Prism4, San Diego, CA) was used to analyze the data. Student's *t*-test or one-way analysis of variance (ANOVA) with post hoc analysis using Turky's multiple comparison test was used for parametric data. Statistical significance was defined as $P < 0.05$.

RESULTS

Effects of ATO on Levels of ROS and GSH Content in Calu-6 Cells

We investigated the levels of ROS in ATO-treated Calu-6 cells. To assess the production of the intracellular H_2O_2 in ATO-treated Calu-6 cells, we used H_2DCFDA fluorescence dye. We first screened Calu-6 cells with the high range concentrations of ATO and various incubation times and chose the optimal range doses of ATO (2–30 μM) and incubation times [early time (10–180 min) and late time (72 h)]. As shown in Figure 1A,B, the intracellular H_2O_2 levels were significantly decreased in Calu-6 cells treated with the indicated concentrations of ATO for 72 h. In contrast, an increase in H_2O_2 levels by this agent was clearly detected within 60 min (Fig. 1C). Maximum generation of H_2O_2 was also reached at 60 min after treatment with 2 μM ATO. The level of H_2O_2 was then decreased after approximately 60 min in Calu-6 cells treated with the tested concentrations of ATO. The levels H_2O_2 in 50 μM ATO-treated cells was decreased to the levels below those observed in control cells at 180 min. The method that was used to detect the intracellular H_2O_2 using the H_2DCFDA fluorescence was considered to be correct, since we were able to clearly observe the increasing DCF fluorescence in the H_2O_2-treated Calu-6 cells in our experimental conditions (data not shown).

Next, we determined the change of the intracellular $O_2^{\cdot -}$ in ATO-treated Calu-6 cells. Red fluorescence derived from DHE, reflecting $O_2^{\cdot -}$ accumulation was significantly increased in Calu-6 cells treated with the indicated concentrations of ATO for 72 h (Fig. 2A,B). The level of the intracellular $O_2^{\cdot -}$ in Calu-6 cells treated with 10 μM ATO was approximately 4.5 times higher than that of the control cells (Fig. 2A,B). The accumulation of $O_2^{\cdot -}$ was observed at an early time point of 10 min in 10 μM ATO-treated Calu-6 cells (Fig. 2C). In case of cells treated with 2 μM ATO, the production of $O_2^{\cdot -}$ was increased at approximately 60 min. The levels of $O_2^{\cdot -}$ were then decreased after approximately 60 min in Calu-6 cells treated with the tested concentrations of ATO. The level of $O_2^{\cdot -}$ in 50 μM ATO-treated cells was not increased during the tested time.

SOD, which catalyzes the dismutation of $O_2^{\cdot -}$ into H_2O_2 and molecular oxygen, is one of the most important antioxidative enzymes. Catalase then metabolizes H_2O_2 to O_2 and H_2O. As shown in Figure 3A, the activity of total SOD and CuZn-SOD were significantly decreased by treatment with indicated amounts of ATO at 72 h while the activity of Mn-SOD was increased by treatment with 10 μM ATO at 72 h. Treatment with ATO significantly decreased the activity of catalase in Calu-6 cells at 72 h (Fig. 3B).

Cellular GSH has been shown to be crucial for regulation of cell proliferation, cell cycle progression and apoptosis [Poot et al., 1995; Schnelldorfer et al., 2000]. Therefore, we analyzed the changes of GSH level in Calu-6 cells using CMF fluorescence. The M1 population of Calu-6 cells showed the lower levels of the intracellular GSH content (Fig. 4A). ATO significantly elevated the percentages of cells residing in the M1 population in a dose-dependent manner at 72 h (Fig. 4A,B), which indicated the depletion of the intracellular GSH content in Calu-6 cells following treatment with ATO. The noteworthy changes in the depletion of the

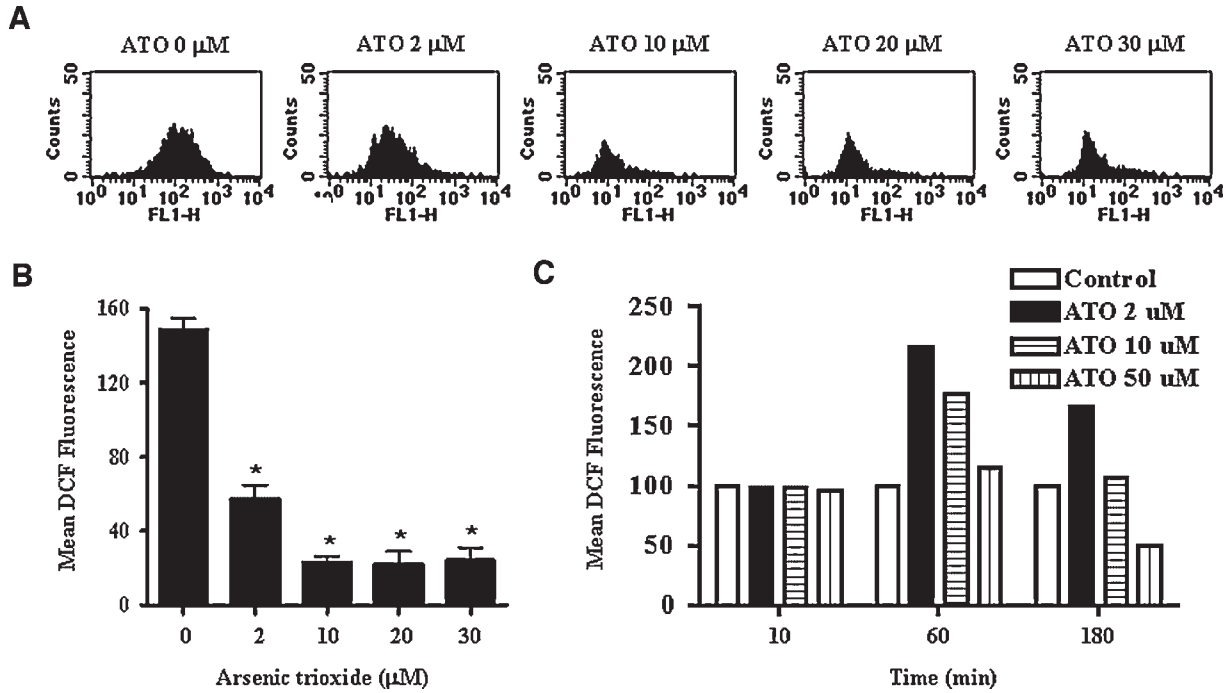

Fig. 1. Effects of ATO on ROS production, H_2O_2 in Calu-6 cells. **A**: Exponentially-growing cells were treated with the indicated amounts of ATO for 72 h. The intracellular H_2O_2 levels were determined by a FACStar flow cytometer as described in Materials and Methods Section. **B**: The graph shows the levels of mean DCF fluorescence of (A). **C**: The graph shows the levels of mean DCF fluorescence in cells for the designated concentration and times. *$P < 0.05$ as compared with the control group cells.

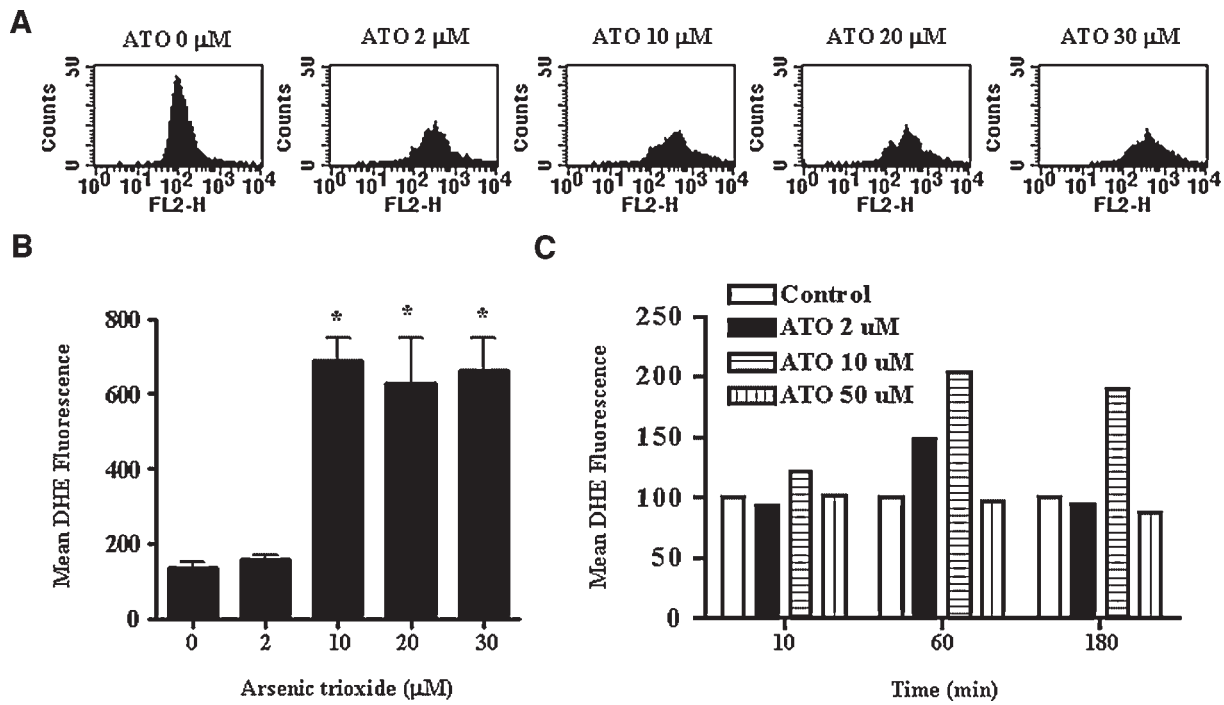

Fig. 2. Effects of ATO on ROS production, $O_2^{\cdot -}$ in Calu-6 cells. **A**: Exponentially-growing cells were treated with the indicated amounts of ATO for 72 h. The intracellular $O_2^{\cdot -}$ levels were determined by a FACStar flow cytometer as described in Materials and Methods Section. **B**: The graph shows the levels of mean DHE fluorescence of (A). **C**: The graph shows the levels of mean DHE fluorescence in cells for the designated concentration and times. *$P < 0.05$ as compared with the control group cells.

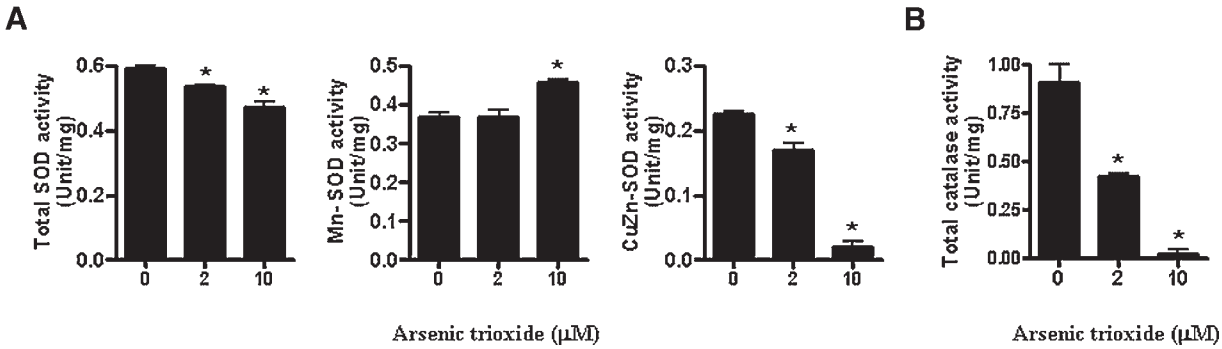

Fig. 3. Effects of ATO on activities of SOD and catalase in Calu-6 cells. Exponentially-growing cells were treated with the indicated amounts of ATO for 72 h. **A**: The graphs show the activity of total SOD, Mn-SOD, and CuZn-SOD in ATO-treated and -untreated Calu-6 cells. **B**: The graph shows the changes of catalase activity by ATO. *$P < 0.05$ as compared with the control group cells.

intracellular GSH content were observed at the concentrations of approximately 2–10 μM ATO. However, the increase of GSH level (mean CMF fluorescence) was slightly observed at 2 μM ATO-treated cells at 72 h (Fig. 4A) and was also observed at an early time point of 10 min in ATO-treated Calu-6 cells (Fig. 4C). Maximum increase in GSH levels was reached at 60 min after treatment with 10 μM ATO. The increase lasted for the tested time of 5 h. Next, to evaluate whether the M1 population of cells in the negative CMF fluorescence region were dead or not, we additionally stained cells with PI for verifying the disruption of the plasma membrane. As shown in Figure 5, the proportion of CMF negative and PI positive cells was

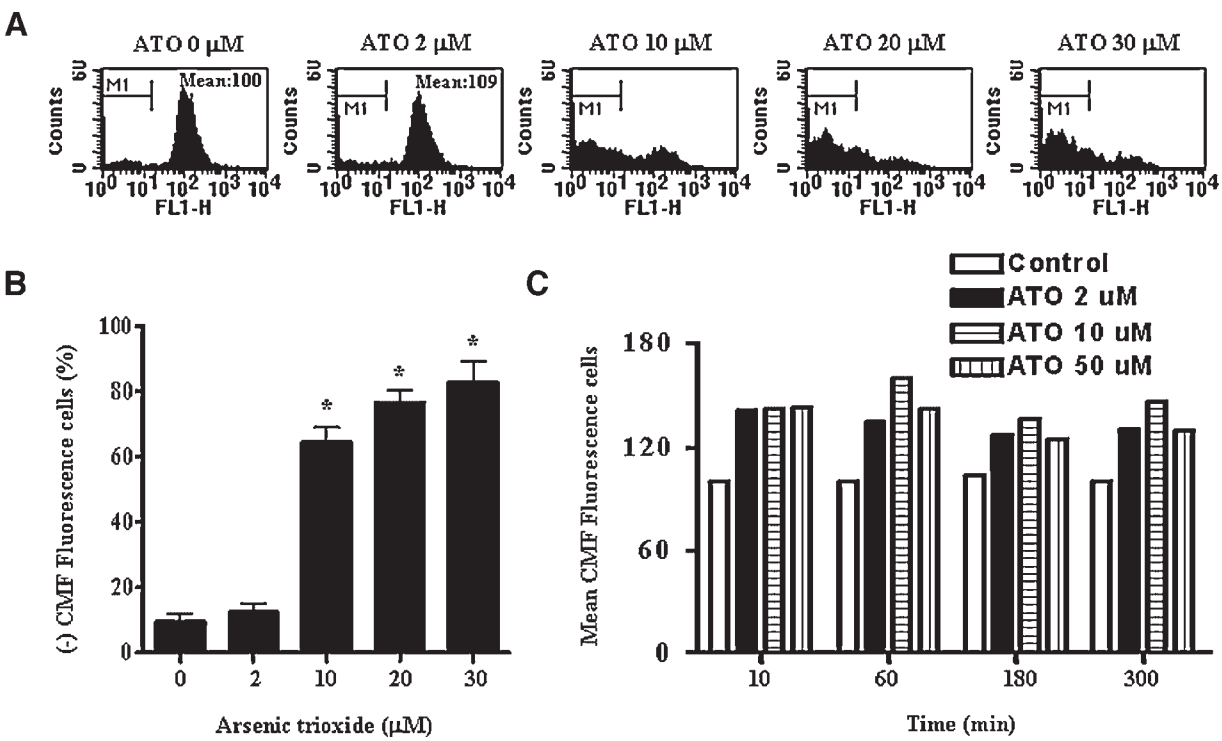

Fig. 4. Effects of ATO on GSH content in Calu-6 cells. Exponentially-growing cells were treated with the indicated amounts of ATO for 72 h. **A**: The intracellular GSH levels were determined by a FACStar flow cytometer as described in Materials and Methods Section. **B**: The graph shows the percent of CMF negative fluorescence (GSH depleted) cells of the M1 region in ATO-treated Calu-6 cells. **C**: The graph shows the levels of mean CMF fluorescence in cells for the designated concentration and times. *$P < 0.05$ as compared with ATO-untreated control group cells.

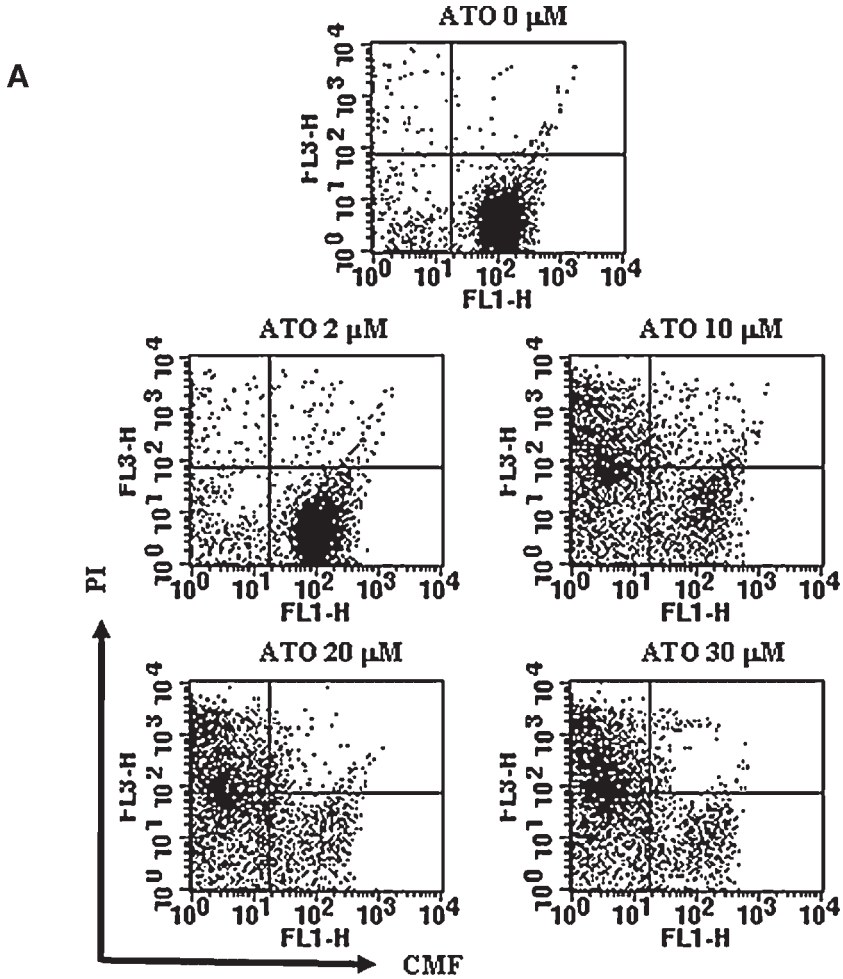

Fig. 5. Effects of ATO on CMF (GSH content) and PI (cell viability) fluorescence in Calu-6 cells. Exponentially-growing cells were treated with the indicated amounts of ATO for 72 h. **A**: CMF fluorescence cells and PI positive staining cells were measured using a FACStar flow cytometer. **B**: The graph shows the percent of CMF negative and PI positive staining cells from the above figures from (A). $^*P < 0.05$ as compared with ATO-untreated control group cells.

increased in a dose-dependent manner. Many of the negative CMF fluorescence cells treated with 30 μM ATO at 72 h showed PI positive staining, which indicated that the cells showing GSH depletion would be generally dead.

Effects of ROS Scavengers on ROS Production, GSH Depletion, and Apoptosis in ATO-Treated Calu-6 Cells

To determine whether ROS production and GSH depletion in ATO-treated Calu-6 cells were changed by ROS scavengers, cell-permeable ROS scavengers, Tempol and Tiron [Yamada et al., 2003], and well-known antioxidants, NAC and rGSHester, were co-incubated with ATO-treated Calu-6 cells for 72 h. An anti-ischemic and metabolic agent, Trimetazidine was also used as an indirect antioxidant [Tikhaze et al., 2000; Stanley and Marzilli, 2003]. To measure the accurate intracellular fluorescence level of ROS, we used only the cells residing in the R2 region (Supplements 1A and B). These cells are considered to have intact plasma membrane. The scavengers of 200 μM concentration except Tempol did not significantly change the intracellular H_2O_2 levels in 10 μM ATO-treated cells at 72 h (Fig. 6A and Supplement 1A). The scavengers of Tempol and NAC reduced the increased $O_2^{\cdot -}$ levels in ATO-treated cells (Fig. 6B and Supplement 1B). However, the treatment of 200 μM Tiron, Trimetazidine and rGSHester did not change the intracellular $O_2^{\cdot -}$ levels in ATO-treated cells. Interestingly, treatment with 2 mM rGSHester intensified the level of $O_2^{\cdot -}$ in ATO-treated Calu-6 cells (Fig. 6B). All of the ROS scavengers used in this experiment did not significantly change the intracellular ROS levels in Calu-6 control cells (data not shown). We did not use 2 mM of Tempol, Tiron, and Trimetazidine in this experiment since this concentration slightly reduced the viability of control cells. It is possible that 2 mM NAC can change ROS levels in ATO-treated Calu-6 cells in the early stage of incubation. According to Supplement 2, treatment with 2 mM NAC slightly reduced the intracellular H_2O_2 levels in ATO-treated cells at 10 min and strongly reduced those in these cells at 180 min. In contrast, treatment with 2 mM did not reduce the intracellular $O_2^{\cdot -}$ levels in ATO-treated cells at 10, 50, and 180 min (Supplement 3). Instead, 2 mM NAC augmented the levels of $O_2^{\cdot -}$ in ATO-treated cells at the early times.

The other scavengers except 2 mM NAC did not inhibit depletion of the GSH content in ATO-treated Calu-6 cells (Fig. 6C and Supplement 1C). In contrast, NAC showed the significant recovery of the depleted GSH content in ATO-treated cells (Fig. 6C and Supplement 1C). Next, we evaluated the changes of the proportion of CMF negative and PI positive cells in ATO-treated cells in the presence of ROS scavenger. As shown in Figure 6D and Supplement 4, ROS scavengers did not significantly change the proportion of CMF negative and PI positive cells. Conversely, treatments with 2 mM NAC decreased the proportion of CMF negative and PI positive cells, indicating that NAC inhibited the disruption of the plasma membrane in ATO-treated cells.

Next, we attempted to examine whether these scavengers inhibited ATO-induced Calu-6 cell death, since ATO induced apoptosis in these cells (unpublished data). The scavengers except 2 mM NAC did not rescue cells from ATO-induced apoptosis (Fig. 7 and Supplement 5). Treatment with 2 mM NAC significantly reduced the levels of apoptosis in ATO-treated cells in view of sub-G1 cells (approximately 25% vs. 37%) (Fig. 7A and Supplement 5A) and annexin V staining cells (approximately 30% vs. 47%) (Fig. 7B and Supplement 5B). In addition, treatment with Tempol and 2 mM NAC prevented the loss of mitochondrial membrane potential ($\Delta\Psi_m$) in ATO-treated Calu-6 cells (Fig. 7C and Supplement 5C). In contrast, treatment with 2 mM rGSHester intensified the loss of that in ATO-treated Calu-6 cells (Fig. 7C).

Effects of SOD and Catalase on ROS Production, GSH Depletion and Apoptosis in ATO-Treated Calu-6 Cells

Next, to determine whether ROS and GSH levels in ATO-treated Calu-6 cells were changed by treatment with exogenous SOD and catalase, Calu-6 cells were treated with ATO in the presence or absence of SOD (30 U/ml) or/and catalase (30 U/ml) for 72 h. As shown in Figure 8A and Supplement 6A, SOD or/and catalase significantly increased the level of H_2O_2 in ATO-treated Calu-6 cells. Treatment with SOD or/and catalase did not alter the H_2O_2 levels in Calu-6 control cells. In regard to $O_2^{\cdot -}$ levels, SOD and/or catalase significantly reduced the $O_2^{\cdot -}$ levels in ATO-treated Calu-6 cells (Fig. 8B and Supplement 6B). When we

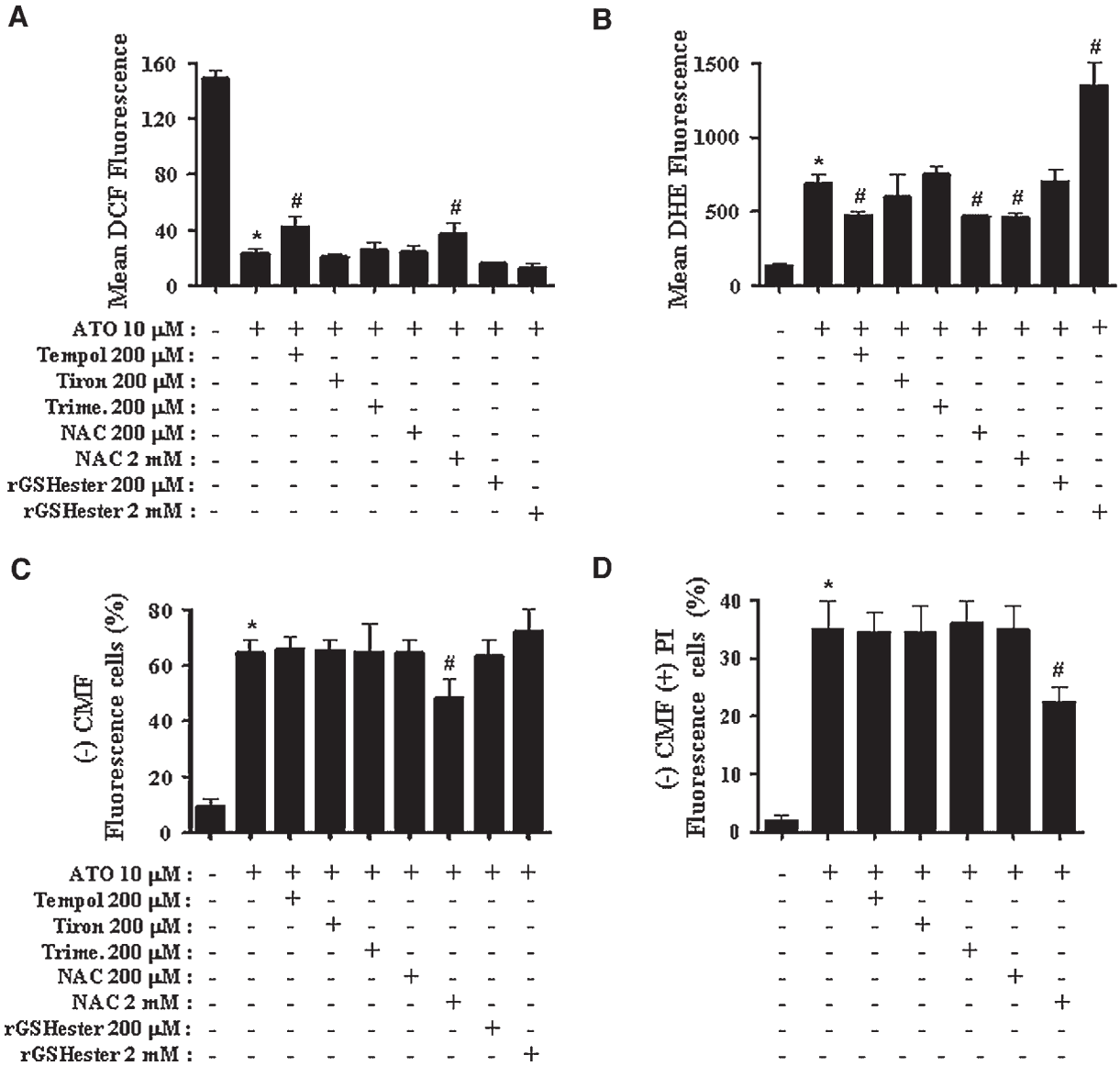

Fig. 6. Effects of ROS scavengers on the intracellular ROS and GSH levels in ATO-treated Calu-6 cells. Exponentially-growing cells were treated with the indicated amounts of ROS scavengers in addition to 10 μM of ATO for 72 h. The graphs show the levels of mean DCF fluorescence (**A**) and mean DHE fluorescence (**B**), the percents of CMF negative fluorescence (GSH depleted) cells (**C**), and the percents of CMF negative and PI positive staining cells (**D**). $^{*}P < 0.05$ as compared with the control group cells. $^{\#}P < 0.05$ as compared with cells treated with only ATO.

assessed the levels of intracellular GSH by SOD and catalase, SOD and/or catalase did not inhibit the depletion of GSH content in Calu-6 cells treated with ATO (Fig. 8C and Supplement 6C). No synergistic or additive effects of SOD and catalase on the levels of ROS and GSH were detected (Fig. 8A–C). In addition, as shown in Figure 8D and Supplement 7, the proportion of CMF negative and PI positive cells in ATO-treated Calu-6 cells was not changed after exposure to SOD and/or catalase.

Next, we examined whether SOD and catalase prevented ATO-induced Calu-6 cell death. None of the SOD and catalase prevented apoptosis in Calu-6 cells treated with ATO (Fig. 9) in view of sub-G1 cells (Fig. 9A and Supplement 8A) and annexin V positive stained cells (Fig. 9B and Supplement 8B). In relation to the mitochondrial membrane potential ($\Delta\Psi_m$), SOD and/or catalase also did not prevent the loss of mitochondrial transmembrane potential ($\Delta\Psi_m$) in ATO-treated Calu-6 cells (Fig. 9C and

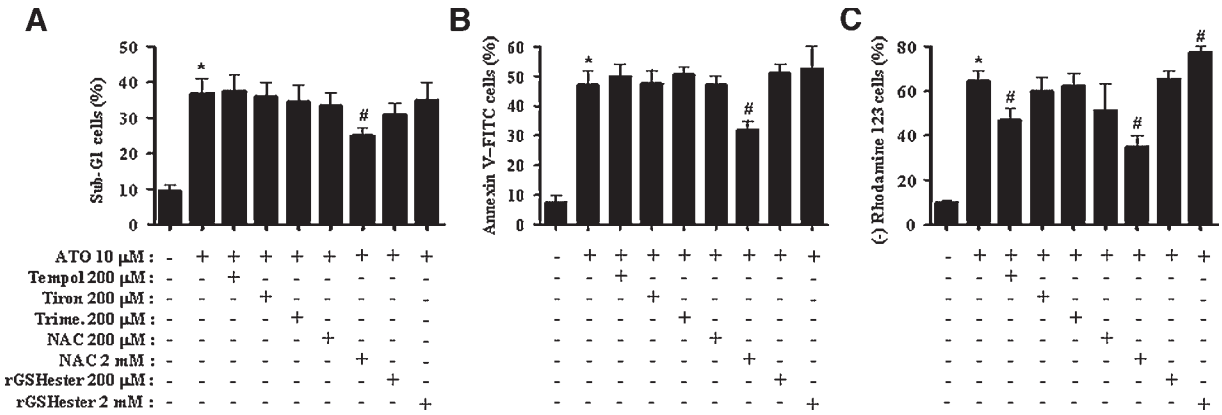

Fig. 7. Effects of ROS scavengers on ATO-induced apoptosis. Exponentially-growing cells were treated with the indicated amounts of ROS scavengers in addition to 10 μM of ATO for 72 h. Sub-G1 cells, annexin positive cells and Rhodamine 123 negative cells were measured using flow cytometric analysis in Materials and Methods Section. The graphs show the percents of sub-G1 cells (**A**), annexin positive cells (**B**), and Rhodamine 123 negative cells (**C**). $^{*}P < 0.05$ as compared with the control group. $^{\#}P < 0.05$ as compared with cells treated with only ATO.

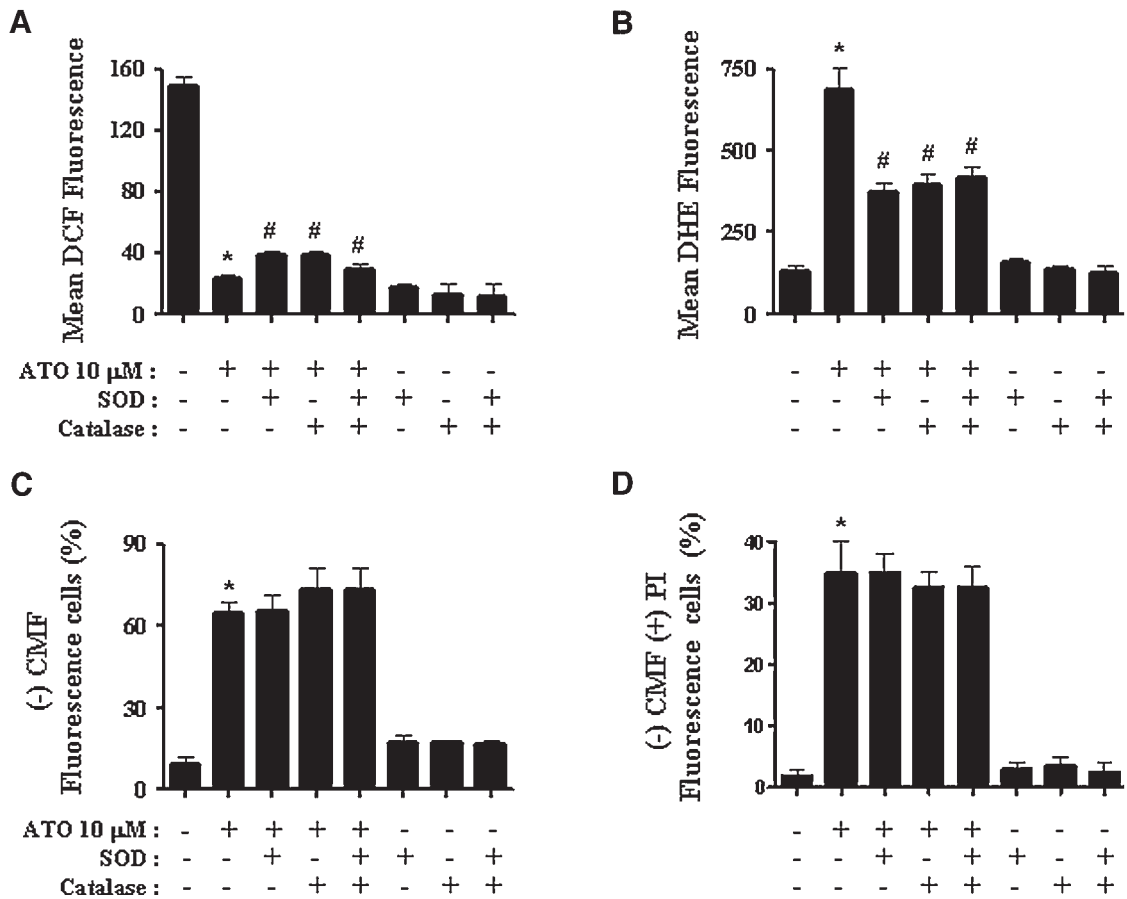

Fig. 8. Effects of SOD and catalase on the intracellular ROS and GSH levels in ATO-treated Calu-6 cells. Exponentially-growing cells were treated with SOD and catalase in addition to ATO for 72 h. The graphs show the levels of mean DCF fluorescence (**A**) and mean DHE fluorescence (**B**), the percent of CMF negative fluorescence (GSH depleted) cells (**C**) and the percents of CMF negative and PI positive staining cells (**D**). $^{*}P < 0.05$ as compared with the control group cells. $^{\#}P < 0.05$ as compared with cells treated with only ATO.

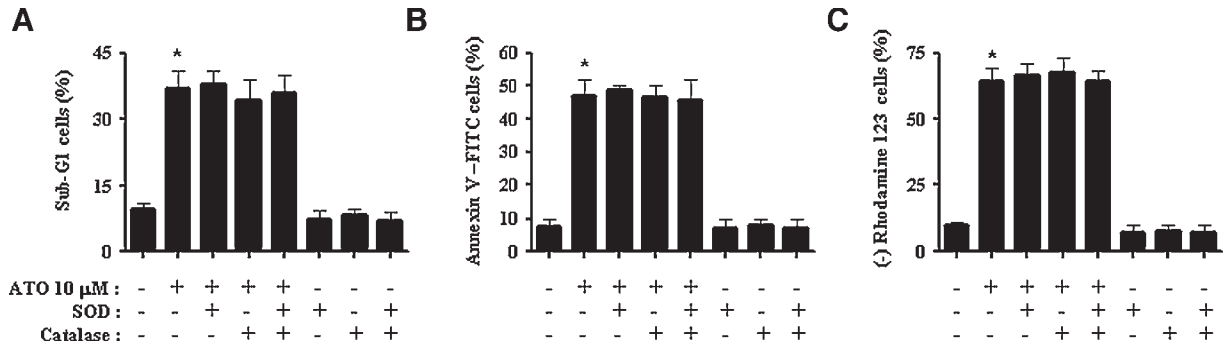

Fig. 9. Effects of SOD and catalase on ATO-induced apoptosis. Exponentially-growing cells were treated with SOD and catalase in addition to ATO for 72 h. Sub-G1 cells, annexin positive cells, and Rhodamine 123 negative cells were measured using flow cytometric analysis in Materials and Methods Section. The graphs show the percent of sub-G1 cells (**A**), annexin positive cells (**B**), and Rhodamine 123 negative cells (**C**). $^{*}P < 0.05$ as compared with the control group cells.

Supplement 8C). SOD and catalase used in this experiment did not significantly change the levels of apoptosis in Calu-6 control cells. SOD (60 U/ml) and/or catalase (60 U/ml) did not alter the levels of apoptosis and mitochondria membrane potential (data not shown).

Effects of BSO on the Levels of ROS, GSH, and Apoptosis in ATO-Treated Calu-6 Cells

We investigated whether BSO (an inhibitor of GSH synthesis; [Bailey, 1998]) changed ROS and GSH and apoptosis in ATO-treated Calu-6 cells. Treatment with 1 μM BSO increased H_2O_2 levels as well as $O_2^{\cdot -}$ levels in 1 μM ATO-treated cells (Fig. 10A,B). BSO decreased further the H_2O_2 levels in 5 or 10 μM ATO-treated Calu-6 cells, but BSO increased the $O_2^{\cdot -}$ levels in 5 μM ATO-treated Calu-6 cells (Fig. 10A,B). Treatment with BSO did not alter ROS levels and GSH depletion in Calu-6 control cells (Fig. 10). BSO significantly depleted GSH content in 1 μM ATO-treated cells and intensified the depletion of GSH content in 5 or 10 μM ATO-treated cells (Fig. 10C).

Next, we investigated the effects of BSO on ATO-induced Calu-6 cell death. Treatment with 1 μM BSO intensified ATO-induced Calu-6 cell viability while this agent did not influence the viability of control cells (Fig. 11A). BSO increased the number of sub-G1 cells and annexin V positive staining cells in ATO-treated Calu-6 cells while this agent did not in control cells (Fig. 11B,C). Concerning the mitochondria membrane potential, treatment with BSO increased the loss of mitochondrial membrane potential ($\Delta\Psi_m$) in ATO-treated Calu-6 cells. However, BSO did not reduce the mitochondrial membrane potential ($\Delta\Psi_m$) in Calu-6 control cells (Fig. 11D).

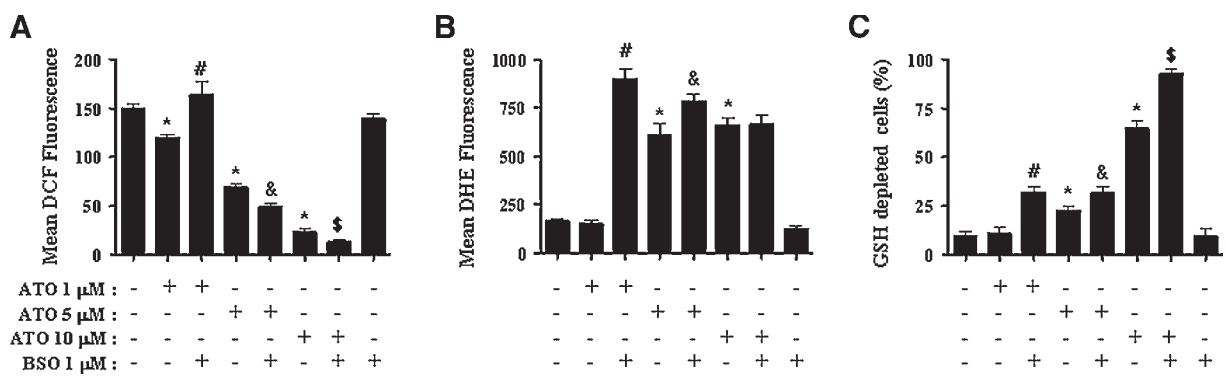

Fig. 10. Effects of BSO on the intracellular ROS and GSH levels in ATO-treated Calu-6 cells. Exponentially-growing cells were treated with 1 or 5 or 10 μM ATO with or without 1 μM BSO for 72 h. The graphs show intracellular H_2O_2 levels (**A**), intracellular $O_2^{\cdot -}$ levels (**B**), and the percents of GSH depleted cells (**C**). $^{*}P < 0.05$ as compared with the ATO-untreated control group cells. $^{\#}P < 0.05$ as compared with the 1 μM ATO-treated group cells. $^{\&}P < 0.05$ as compared with the 5 μM ATO-treated group cells. $^{\$}P < 0.05$ as compared with the 10 μM ATO-treated group cells.

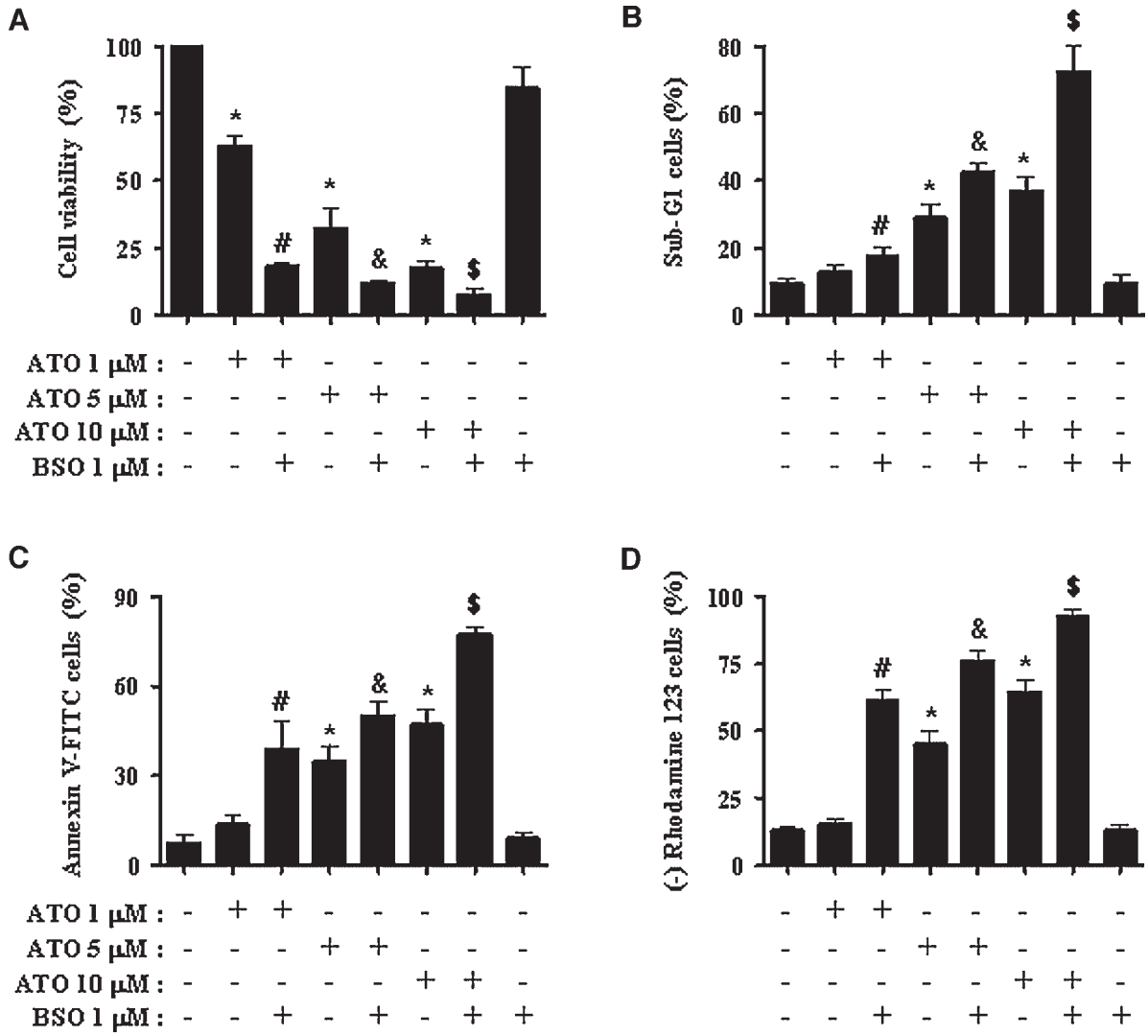

Fig. 11. Effects of BSO on cell viability and apoptosis in ATO-treated Calu-6 cells. Exponentially-growing cells were treated with 1 or 5 or 10 μM ATO with or without 1 μM BSO for 72 h. **A**: Cell viability was assessed by MTT assays, (**B**) sub-G1 cells, (**C**) annexin V staining cells, and (**D**) Rhodamine 123 negative staining cells were measured with a FACStar flow cytometer. $^{*}P < 0.05$ as compared with the ATO-untreated control group cells. $^{\#}P < 0.05$ as compared with the 1 μM ATO-treated group cells. $^{\&}P < 0.05$ as compared with the 5 μM ATO-treated group cells. $^{\$}P < 0.05$ as compared with the 10 μM ATO-treated group cells.

DISCUSSION

In this study, we focused on the involvement of ROS such as H_2O_2 and $O_2^{\cdot -}$, and GSH in ATO-induced Calu-6 cell death, since we have previously found that ATO inhibited the growth of Calu-6 cells with an IC_{50} of approximately 3–4 μM at 72 h, and 10 μM ATO inhibited the growth of Calu-6 cells about 80% using a MTT assay and induced apoptosis about 40% (unpublished data). In this experiment, we used a concentration of 10 μM ATO. This concentration was considered to be suitable dose to differentiate the levels of apoptosis in the presence of ATO versus apoptosis in the presence of ATO and ROS scavengers such as SOD and catalase.

ATO can disturb the natural oxidation and reduction equilibrium in cells, leading to an increase of ROS by a variety of redox enzymes, including flavoprotein-dependent superoxide-producing enzymes such as NADPH oxidase [Miller et al., 2002; Chou et al., 2004; Kim et al., 2006; Li et al., 2006]. ATO decreases glutathione (GSH) levels and increases intracellular ROS levels in certain APL cells [Dai et al., 1999]. Therefore, to elucidate the involvement of ROS such as H_2O_2 and $O_2^{\cdot -}$ in ATO-induced Calu-6

cell death, we assessed these ROS levels by using H_2DCFDA and DHE fluorescence. Our data showed that the intracellular H_2O_2 level was significantly decreased in ATO-treated Calu-6 cells at 72 h. Since treatment with 1–2 μM ATO did not significantly induce cell death, the lower value of DCF fluorescence in ATO-treated cells is not due to leakage of DCF dye from cells. This result is not consistent with other reports, which indicated that increased intracellular H_2O_2 played an important role in ATO-induced cell death in cervical cancer cells [Kang et al., 2004], APL cells [Jing et al., 1999], hepatocellular carcinoma HepG2 [Li et al., 2006], and glioblastoma A172 cells [Haga et al., 2005]. However, there was an increase in intracellular H_2O_2 levels within 60 min in 2 or 10 μM ATO-treated Calu-6 cells. Data from Haga et al. [2005] also showed that H_2O_2 accumulation was detected in ATO-treated glioblastoma T98G cells, but apoptosis did not occur in these cells. These discrepancies likely result from cell-type specificity and the differences of incubation times. According to our current data, treatment with 10 μM ATO induced apoptosis in Calu-6 cells without an increase in intracellular H_2O_2 levels, as evidenced by sub-G1 cells and annexin V-staining cells. In addition, the lower doses of ATO (1 or 5 μM) increased the H_2O_2 levels regardless of the viability of other lung cancer cell line, A549, while the higher doses of ATO (20, 30, or 50 μM) decreased the H_2O_2 levels along with the reduction of A549 cell viability (Supplements 9A and D). Furthermore, treatment with 2 mM NAC showing the significant inhibition in ATO-induced apoptosis increased the intracellular H_2O_2 levels. However, Tempol, SOD, and catalase increased the intracellular H_2O_2 levels in ATO-treated cells without the effect on apoptosis. In addition, BSO increased or decreased the intracellular H_2O_2 levels in Calu-6 cells depending on concentration of ATO, but BSO enhanced the levels of apoptosis in these cells. Our data suggest that the apoptotic effects of ATO are not comparative to the intracellular H_2O_2 levels in Calu-6 cells. However, we cannot rule out the possibility that the increased H_2O_2 levels following treatment with ATO influence on the cells at an early time point to trigger apoptosis, since we were able to detect an increase in intracellular H_2O_2 levels within 60 min in 2 or 10 μM ATO-treated Calu-6 cells and to observe that 2 mM NAC reduced the increased H_2O_2 levels in ATO-treated Calu-6 cells at the early time points.

It have been reported that the increased pattern of $O_2^{\cdot -}$ by ATO was reported in esophageal cancer SHEE85 cells [Shen et al., 2003] but this pattern was not observed in ATO-treated acute myelogenous leukemia HL-60 cells [Han et al., 2005], renal cell carcinoma ACHN cells [Wu et al., 2004] and HeLa cervical cancer (unpublished data). These discrepancies also may result from different cell-type. According to our result, treatment with ATO increased or decreased the intracellular $O_2^{\cdot -}$ levels in A549 lung cancer cells (Supplement 9) and markedly enhanced the production of $O_2^{\cdot -}$ in Calu-6 cells at 72 h. It is possible that the increased $O_2^{\cdot -}$ levels in ATO-treated Calu-6 cells result from the enhanced production of $O_2^{\cdot -}$ itself and/or the reduction of SOD activity. An early response to ATO probably enhanced production of $O_2^{\cdot -}$ itself since $O_2^{\cdot -}$ levels were increased and decreased by ATO in the short time period. The changes of $O_2^{\cdot -}$ levels seem to result in the increase and decrease of H_2O_2 levels in ATO-treated cells at the early time phases. The high levels of $O_2^{\cdot -}$ in ATO-treated cells at 72 h were likely to be from the decreased activity of SOD, especially CuZn-SOD activity, as well as enhanced production of $O_2^{\cdot -}$ itself. Interestingly, an increase in Mn-SOD activity was observed in 10 μM ATO-treated cells. This increase seems to dismutate the superoxide radical ($O_2^{\cdot -}$) generated from mitochondria into H_2O_2. Therefore, it is possible that the reduction of SOD activity results in the decreased H_2O_2 levels in Calu-6 cells at 72 h. Although ATO also significantly inhibited the activity of catalase at 72 h (Fig. 3B), the H_2O_2 levels was not increased. A decrease in H_2O_2 levels in ATO-treated cell is not probably due to catalase activity, but due to SOD activity and/or other enzymes such as GSH peroxide.

We attempted to determine whether ROS scavengers prevent the ATO-induced cell death through the reduction of the intracellular $O_2^{\cdot -}$ level. Tempol and NAC decreased the level of $O_2^{\cdot -}$ in Calu-6 cells treated with 10 μM ATO at 72 h. Interestingly, 2 mM NAC did not reduce the levels of $O_2^{\cdot -}$ in ATO-treated cells at the early time phases (Supplement 3). This result suggests and supports the hypothesis that the immediate effect of NAC could be prooxidant and the delayed effect of NAC could be antioxidant in cells [Menon et al., 2007]. Treatment

with Tiron and Trimetazidine did not reduce the levels. Probably, the weak abilities of these scavengers, especially Tiron as a $O_2^{\cdot -}$ scavenger may be due to the lower dose of these or/and the long time incubation, since Yamada et al. [2003] showed that the effects of Tiron on reduction in $O_2^{\cdot -}$ level occurred at 3 h and at more than 1 mM concentration of Tiron in pyrogallol-treated PC12 cells. Although NAC reduced the levels of $O_2^{\cdot -}$ in Calu-6 cells treated with 10 μM ATO, treatment with the higher dose of NAC (2 mM) only significantly inhibited apoptosis in ATO-treated cells, as evidenced by sub-G1 cells, annexin V staining cells and the loss of mitochondrial transmembrane potential ($\Delta\Psi_m$). In addition, Tempol strongly prevented the loss of mitochondrial transmembrane potential ($\Delta\Psi_m$), suggesting that Tempol play a role in protection of mitochondrial transmembrane potential ($\Delta\Psi_m$) rather than in inhibition of apoptosis. In contrast, treatment with 2 mM rGSHester showing an increased effect on the level of $O_2^{\cdot -}$ in ATO-treated Calu-6 cells intensified the loss of mitochondrial transmembrane potential ($\Delta\Psi_m$) in these cells. SOD and catalase used in our experiment significantly reduced the $O_2^{\cdot -}$ levels in ATO-treated cells. However, both of them did not prevent apoptosis induced by ATO. In addition, BSO increased the $O_2^{\cdot -}$ levels in 1 or 5 μM ATO-treated cells along with enhancement of apoptosis while BSO did not increase the $O_2^{\cdot -}$ levels in 10 μM ATO-treated cells along with enhancement of apoptosis (Figs. 10B and 11). In relation to A549 cells, the lower doses of ATO (1 or 5 μM) increased the $O_2^{\cdot -}$ levels without reduction of A549 cell viability (Supplements 9B and D). Taken together, these results suggest that the changes of intracellular $O_2^{\cdot -}$ level are not entirely but are at least partially correlated to apoptosis in ATO-treated Calu-6 cells. These data also suggest that besides the changes of intracellular level of ROS, other redox regulators such as GSH are required for explaining the ATO-induced apoptosis in Calu-6 cells.

It has been reported that the intracellular GSH content has a decisive effect on anticancer drug-induced apoptosis, indicating that apoptotic effects are inversely comparative to GSH content [Kito et al., 2002; Pu et al., 2002; Higuchi, 2004; Maeda et al., 2004; Estrela et al., 2006; Ramos et al., 2006]. The intracellular GSH content also has a decisive effect on ATO-induced apoptosis [Dai et al., 1999; Kitamura et al., 2000; Wu et al., 2004; Li et al., 2006]. Likewise, our result clearly indicated the depletion of intracellular GSH content by ATO in Calu-6 and A549 (Supplement 9C) cancer cells at 72 h. Conversely, the increase of GSH content was observed in 2 μM ATO-treated cells at 72 h and in ATO-treated Calu-6 cells at the early time points of incubation. This result was likely due to the defense action of Calu-6 cells against the toxin of ATO at the earlier time points. No effect of Tempol, Tiron, Trimetazidine, SOD, and catalase on preventing apoptosis in ATO-treated cells likely resulted from the failure of the recovery of GSH depletion induced by ATO. We have also shown that many of the negative CMF fluorescence (GSH depletion) cells were considered to be dead, as evidenced by PI positive staining. Not 200 μM NAC and rGSHester but 2 mM NAC showing significantly the recovery of GSH depletion was found to decrease PI positive cells and to reduced levels of apoptosis in ATO-treated Calu-6 cells. In addition, as expected, BSO increased the GSH depletion and apoptosis in ATO-treated cells. It has been reported that the therapeutic range of ATO in cancer treatment is 1–2 μM [Dai et al., 1999; Miller et al., 2002]. Interestingly, treatment with 1 μM BSO or 1 μM ATO alone did not deplete GSH content and induce apoptosis in Calu-6 cells, while combined treatment with both agents scientifically depleted GSH content and induced apoptosis in these cells. This positive result can prompt additional investigations in other lung cancer or in animal model using this combination of BSO and ATO. Taken together, these results support that the intracellular GSH levels are tightly related to ATO-induced cell death. However, the present result related to treatment with 2 mM rGSHester in 10 μM ATO-treated cells may appear as contradictory with previous many reports [Dai et al., 1999; Kitamura et al., 2000; Kito et al., 2002; Pu et al., 2002; Maeda et al., 2004; Wu et al., 2004; Li et al., 2006; Ramos et al., 2006] as well as our result related to NAC treatment. Unfortunately, these papers did not use rGSHester in ATO-treated cells but used NAC and/or BSO to suggest that the changes of GSH content are involved in ATO-induced cell death. Similar to our result, Piga et al. [2007] demonstrated that treatment with NAC but not GSH inhibited PC12 cell death induced by ATO. They explained no inhibitory effect of GSH by suggesting that exogenous GSH is not easily

incorporated into cells. However, rGSHester used in this experiment is known to enter easily into cells. We cannot exactly explain non-effect of rGSHester on the inhibition of ATO-induced cell death. Of note, ATO is known to be directly quenched by thiols such as NAC and GSH in aqueous solution at neutral pH [Scott et al., 1993]. Therefore, it is possible that NAC scavengered ATO more strongly than GSH did in this experiment. Whatever the mechanism involved, it may be reasonable to assume that the intracellular GSH levels are at least in part related to ATO-induced cell death, and the GSH depletion in ATO-treated cells is accompanied by their death.

In summary, ATO strongly generated $O_2^{\cdot -}$ and induced the depletion of GSH content in Calu-6 cells. Treatment with NAC significantly rescued cells from ATO-induced apoptosis throughout the recovery of GSH depletion while treatment with BSO significantly increased the depletion of content and apoptosis in ATO-treated cells. Our results suggest that ATO induces apoptosis in Calu-6 cells via the depletion of the intracellular GSH contents rather than the changes of ROS levels.

ACKNOWLEDGMENTS

This research was supported by the Korea Research Foundation Grant funded by the Korean Government (MOEHRD) and the Korean Science and Engineering Foundation (R01-2006-000-10544-0).

REFERENCES

Bailey HH. 1998. L-S,R-buthionine sulfoximine: Historical development and clinical issues. Chem Biol Interact 111–112:239–254.

Baj G, Arnulfo A, Deaglio S, Mallone R, Vigone A, De Cesaris MG, Surico N, Malavasi F, Ferrero E. 2002. Arsenic trioxide and breast cancer: Analysis of the apoptotic, differentiative and immunomodulatory effects. Breast Cancer Res Treat 73:61–73.

Baran CP, Zeigler MM, Tridandapani S, Marsh CB. 2004. The role of ROS and RNS in regulating life and death of blood monocytes. Curr Pharm Des 10:855–866.

Bubici C, Papa S, Pham CG, Zazzeroni F, Franzoso G. 2006. The NF-kappaB-mediated control of ROS and JNK signaling. Histol Histopathol 21:69–80.

Chen TJ, Jeng JY, Lin CW, Wu CY, Chen YC. 2006. Quercetin inhibition of ROS-dependent and -independent apoptosis in rat glioma C6 cells. Toxicology 223:113–126.

Chou WC, Jie C, Kenedy AA, Jones RJ, Trush MA, Dang CV. 2004. Role of NADPH oxidase in arsenic-induced reactive oxygen species formation and cytotoxicity in myeloid leukemia cells. Proc Natl Acad Sci USA 101:4578–4583.

Dai J, Weinberg RS, Waxman S, Jing Y. 1999. Malignant cells can be sensitized to undergo growth inhibition and apoptosis by arsenic trioxide through modulation of the glutathione redox system. Blood 93:268–277.

Dasmahapatra G, Rahmani M, Dent P, Grant S. 2006. The tyrphostin adaphostin interacts synergistically with proteasome inhibitors to induce apoptosis in human leukemia cells through a reactive oxygen species (ROS)-dependent mechanism. Blood 107:232–240.

Estrela JM, Ortega A, Obrador E. 2006. Glutathione in cancer biology and therapy. Crit Rev Clin Lab Sci 43: 143–181.

Haga N, Fujita N, Tsuruo T. 2005. Involvement of mitochondrial aggregation in arsenic trioxide (As2O3)-induced apoptosis in human glioblastoma cells. Cancer Sci 96:825–833.

Han SS, Kim K, Hahm ER, Park CH, Kimler BF, Lee SJ, Lee SH, Kim WS, Jung CW, Park K, Kim J, Yoon SS, Lee JH, Park S. 2005. Arsenic trioxide represses constitutive activation of NF-kappaB and COX-2 expression in human acute myeloid leukemia, HL-60. J Cell Biochem 94:695–707.

Hedley DW, Chow S. 1994. Evaluation of methods for measuring cellular glutathione content using flow cytometry. Cytometry 15:349–358.

Higuchi Y. 2004. Glutathione depletion-induced chromosomal DNA fragmentation associated with apoptosis and necrosis. J Cell Mol Med 8:455–464.

Hyun Park W, Hee Cho Y, Won Jung C, Oh Park J, Kim K, Hyuck Im Y, Lee MH, Ki Kang W, Park K. 2003. Arsenic trioxide inhibits the growth of A498 renal cell carcinoma cells via cell cycle arrest or apoptosis. Biochem Biophys Res Commun 300:230–235.

Jing Y, Dai J, Chalmers-Redman RM, Tatton WG, Waxman S. 1999. Arsenic trioxide selectively induces acute promyelocytic leukemia cell apoptosis via a hydrogen peroxide-dependent pathway. Blood 94:2102–2111.

Kang YH, Yi MJ, Kim MJ, Park MT, Bae S, Kang CM, Cho CK, Park IC, Park MJ, Rhee CH, Hong SI, Chung HY, Lee YS, Lee SJ. 2004. Caspase-independent cell death by arsenic trioxide in human cervical cancer cells: Reactive oxygen species-mediated poly(ADP-ribose) polymerase-1 activation signals apoptosis-inducing factor release from mitochondria. Cancer Res 64:8960–8967.

Kim HR, Kim EJ, Yang SH, Jeong ET, Park C, Kim SJ, Youn MJ, So HS, Park R. 2006. Combination treatment with arsenic trioxide and sulindac augments their apoptotic potential in lung cancer cells through activation of caspase cascade and mitochondrial dysfunction. Int J Oncol 28:1401–1408.

Kitamura K, Minami Y, Yamamoto K, Akao Y, Kiyoi H, Saito H, Naoe T. 2000. Involvement of CD95-independent caspase 8 activation in arsenic trioxide-induced apoptosis. Leukemia 14:1743–1750.

Kito M, Akao Y, Ohishi N, Yagi K, Nozawa Y. 2002. Arsenic trioxide-induced apoptosis and its enhancement by buthionine sulfoximine in hepatocellular carcinoma cell lines. Biochem Biophys Res Commun 291:861–867.

Lauterburg BH. 2002. Analgesics and glutathione. Am J Ther 9:225–233.

Li M, Cai JF, Chiu JF. 2002. Arsenic induces oxidative stress and activates stress gene expressions in cultured lung epithelial cells. J Cell Biochem 87:29–38.

Li JJ, Tang Q, Li Y, Hu BR, Ming ZY, Fu Q, Qian JQ, Xiang JZ. 2006. Role of oxidative stress in the apoptosis of hepatocellular carcinoma induced by combination of arsenic trioxide and ascorbic acid. Acta Pharmacol Sin 27:1078–1084.

Macho A, Hirsch T, Marzo I, Marchetti P, Dallaporta B, Susin SA, Zamzami N, Kroemer G. 1997. Glutathione depletion is an early and calcium elevation is a late event of thymocyte apoptosis. J Immunol 158:4612–4619.

Maeda H, Hori S, Ohizumi H, Segawa T, Kakehi Y, Ogawa O, Kakizuka A. 2004. Effective treatment of advanced solid tumors by the combination of arsenic trioxide and L-buthionine-sulfoximine. Cell Death Differ 11:737–746.

Menon SG, Sarsour EH, Kalen AL, Venkataraman S, Hitchler MJ, Domann FE, Oberley LW, Goswami PC. 2007. Superoxide signaling mediates N-acetyl-L-cysteine-induced G1 arrest: Regulatory role of cyclin D1 and manganese superoxide dismutase. Cancer Res 67: 6392–6399.

Miller WH, Jr., Schipper HM, Lee JS, Singer J, Waxman S. 2002. Mechanisms of action of arsenic trioxide. Cancer Res 62:3893–3903.

Nakagawa Y, Akao Y, Morikawa H, Hirata I, Katsu K, Naoe T, Ohishi N, Yagi K. 2002. Arsenic trioxide-induced apoptosis through oxidative stress in cells of colon cancer cell lines. Life Sci 70:2253–2269.

Oketani M, Kohara K, Tuvdendorj D, Ishitsuka K, Komorizono Y, Ishibashi K, Arima T. 2002. Inhibition by arsenic trioxide of human hepatoma cell growth. Cancer Lett 183:147–153.

Park WH, Seol JG, Kim ES, Hyun JM, Jung CW, Lee CC, Kim BK, Lee YY. 2000. Arsenic trioxide-mediated growth inhibition in MC/CAR myeloma cells via cell cycle arrest in association with induction of cyclin-dependent kinase inhibitor, p21, and apoptosis. Cancer Res 60:3065–3071.

Piga R, Saito Y, Yoshida Y, Niki E. 2007. Cytotoxic effects of various stressors on PC12 cells: Involvement of oxidative stress and effect of antioxidants. Neurotoxicology 28: 67–75.

Poot M, Teubert H, Rabinovitch PS, Kavanagh TJ. 1995. De novo synthesis of glutathione is required for both entry into and progression through the cell cycle. J Cell Physiol 163:555–560.

Pu YS, Hour TC, Chen J, Huang CY, Guan JY, Lu SH. 2002. Cytotoxicity of arsenic trioxide to transitional carcinoma cells. Urology 60:346–350.

Ramos AM, Fernandez C, Amran D, Esteban D, de Blas E, Palacios MA, Aller P. 2006. Pharmacologic inhibitors of extracellular signal-regulated kinase (ERKs) and c-Jun NH(2)-terminal kinase (JNK) decrease glutathione content and sensitize human promonocytic leukemia cells to arsenic trioxide-induced apoptosis. J Cell Physiol 209:1006–1015.

Rigo A, Stevanato R, Viglino P. 1977. Competitive inhibition of Cu, Zn superoxide dismutase by monovalent anions. Biochem Biophys Res Commun 79:776–783.

Schnelldorfer T, Gansauge S, Gansauge F, Schlosser S, Beger HG, Nussler AK. 2000. Glutathione depletion causes cell growth inhibition and enhanced apoptosis in pancreatic cancer cells. Cancer 89:1440–1447.

Scott N, Hatlelid KM, MacKenzie NE, Carter DE. 1993. Reactions of arsenic(III) and arsenic(V) species with glutathione. Chem Res Toxicol 6:102–106.

Seol JG, Park WH, Kim ES, Jung CW, Hyun JM, Kim BK, Lee YY. 1999. Effect of arsenic trioxide on cell cycle arrest in head and neck cancer cell line PCI-1. Biochem Biophys Res Commun 265:400–404.

Shen ZY, Shen WY, Chen MH, Shen J, Zeng Y. 2003. Reactive oxygen species and antioxidants in apoptosis of esophageal cancer cells induced by As2 O3. Int J Mol Med 11:479–484.

Simon HU, Haj-Yehia A, Levi-Schaffer F. 2000. Role of reactive oxygen species (ROS) in apoptosis induction. Apoptosis 5:415–418.

Soignet SL, Maslak P, Wang ZG, Jhanwar S, Calleja E, Dardashti LJ, Corso D, DeBlasio A, Gabrilove J, Scheinberg DA, Pandolfi PP, Warrell RP, Jr. 1998. Complete remission after treatment of acute promyelocytic leukemia with arsenic trioxide. N Engl J Med 339: 1341–1348.

Stanley WC, Marzilli M. 2003. Metabolic therapy in the treatment of ischaemic heart disease: The pharmacology of trimetazidine. Fundam Clin Pharmacol 17:133–145.

Tikhaze AK, Lankin VZ, Zharova EA, Kolycheva SV. 2000. Trimetazidine as indirect antioxidant. Bull Exp Biol Med 130:951–953.

Uslu R, Sanli UA, Sezgin C, Karabulut B, Terzioglu E, Omay SB, Goker E. 2000. Arsenic trioxide-mediated cytotoxicity and apoptosis in prostate and ovarian carcinoma cell lines. Clin Cancer Res 6:4957–4964.

Wallach-Dayan SB, Izbicki G, Cohen PY, Gerstl-Golan R, Fine A, Breuer R. 2006. Bleomycin initiates apoptosis of lung epithelial cells by ROS but not by Fas/FasL pathway. Am J Physiol Lung Cell Mol Physiol 290:L790–L796.

Wang ZG, Rivi R, Delva L, Konig A, Scheinberg DA, Gambacorti-Passerini C, Gabrilove JL, Warrell RP, Jr., Pandolfi PP. 1998. Arsenic trioxide and melarsoprol induce programmed cell death in myeloid leukemia cell lines and function in a PML and PML-RARalpha independent manner. Blood 92:1497–1504.

Wilcox CS. 2002. Reactive oxygen species: Roles in blood pressure and kidney function. Curr Hypertens Rep 4: 160–166.

Woo SH, Park IC, Park MJ, Lee HC, Lee SJ, Chun YJ, Lee SH, Hong SI, Rhee CH. 2002. Arsenic trioxide induces apoptosis through a reactive oxygen species-dependent pathway and loss of mitochondrial membrane potential in HeLa cells. Int J Oncol 21:57–63.

Wu XX, Ogawa O, Kakehi Y. 2004. Enhancement of arsenic trioxide-induced apoptosis in renal cell carcinoma cells by L-buthionine sulfoximine. Int J Oncol 24:1489–1497.

Yamada J, Yoshimura S, Yamakawa H, Sawada M, Nakagawa M, Hara S, Kaku Y, Iwama T, Naganawa T, Banno Y, Nakashima S, Sakai N. 2003. Cell permeable ROS scavengers, Tiron and Tempol, rescue PC12 cell death caused by pyrogallol or hypoxia/reoxygenation. Neurosci Res 45:1–8.

Zhang W, Ohnishi K, Shigeno K, Fujisawa S, Naito K, Nakamura S, Takeshita K, Takeshita A, Ohno R. 1998. The induction of apoptosis and cell cycle arrest by arsenic trioxide in lymphoid neoplasms. Leukemia 12:1383–1391.

Zhang TC, Cao EH, Li JF, Ma W, Qin JF. 1999. Induction of apoptosis and inhibition of human gastric cancer MGC-803 cell growth by arsenic trioxide. Eur J Cancer 35:1258–1263.

Zorov DB, Juhaszova M, Sollott SJ. 2006. Mitochondrial ROS-induced ROS release: An update and review. Biochim Biophys Acta 1757:509–517.